Elemental content allometries and silicon uptake rates of planktonic Rhizaria: insights into their ecology and role in biogeochemical cycles – Supporting Information

Manon Laget[1], Natalia Llopis-Monferrer[2], Jean-François Maguer[2], Aude Leynaert[2], Tristan Biard[1]

[1] LOG, Laboratoire d'Océanologie et de Géosciences, Univ. Littoral Côte d'Opale, Univ. Lille, CNRS, IRD, UMR 8187, Wimereux, France.
[2] Univ. Brest, CNRS, IRD, Ifremer, LEMAR, F-29280, Plouzané, France

1 Sampling details

Table 1: Sampling nets used during the CCE-LTER P2107 cruise

Date	Latitude	Longitude	Gear	Depth range (m)
14/07/2021	33.8064	-120.4189	MOCNESS	400-600
17/07/2021	36.2005	-123.036	DeepNet	700-1000
17/07/2021	36.5122	-122.273	DeepNet	300-500
18/07/2021	36.5196	-122.2968	MOCNESS	400-600
21/07/2021	35.7467	-121.6759	RingNet	0-400
23/07/2021	36.1346	-122.102	BongoNet	0-500
24/07/2021	36.1927	-122.4567	RingNet	0-500
27/07/2021	36.0881	-122.3225	MOCNESS	300-600
28/07/2021	36.316	-122.7499	MOCNESS	350-450

2 Image analysis

Table 2: Assigned shapes for rhizarian taxa

Group	Taxon	Shape
Radiolaria	Spumellaria	cylinder
	Phlebarachnium sp.	prolate ellipsoid
	Oroscena sp.	prolate ellipsoid
	Cytocladus sp.	sphere
	solitary Collodaria	sphere
Phaeodaria	Aulacanthidae	sphere
	Aulosphaeridae	sphere
	Castanellidae	sphere
	Tuscaroridae	prolate ellipsoid
	Coelodendridae	sphere
	Medusettidae	sphere or sum of spheres for colonies
	Protocystis sp. (type 1)	prolate ellipsoid
	Protocystis sp. (type 2)	sphere

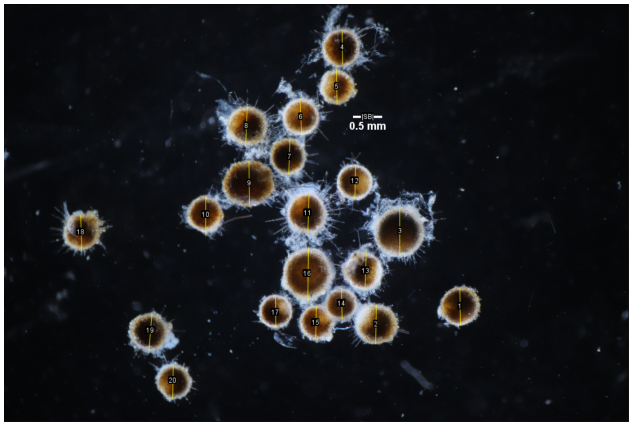

(a) Sample of Castanellidae

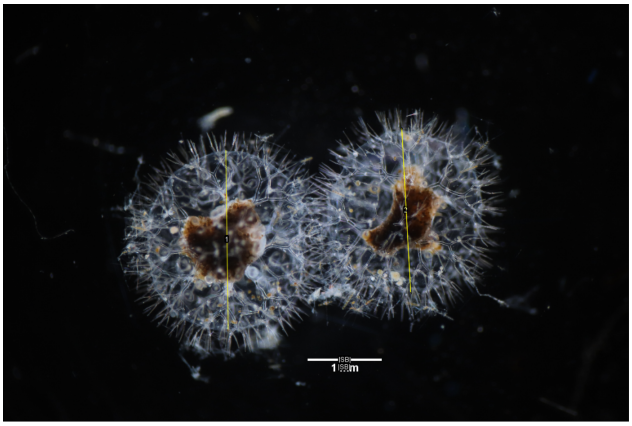

(b) Sample of Coelodendridae

Figure 1: Light microscopy photographs of Rhizaria specimens to describe the methodology for cell measurements

For non spherical objects, the Equivalent Spherical Diameter (ESD) was computed from the volume V as:

$$ESD = \left(\frac{3}{4} \times \frac{V}{\pi}\right)^{\frac{1}{3}} \times 2 \tag{1}$$

3 Silica data from literature

Table 3: Biogenic silica content data available from literature

Type	Mean cell vol. (mm)	nmol Si cell^{-1}	μg Si cell^{-1}	Area*	Reference
Aulacanthidae CCE	0.1	12.46	0.83	CCE	Biard et al., 2018
Aulacanthidae CCE	0.13	13.85	0.93	CCE	Biard et al., 2018

Aulacanthidae CCE	0.08	7.48	0.5	CCE	Biard et al., 2018
Aulacanthidae CCE	0.07	7.21	0.48	CCE	Biard et al., 2018
Aulacanthidae CCE	0.14	52.5	3.52	CCE	Biard et al., 2018
Aulacanthidae CCE	0.1	11.67	0.78	CCE	Biard et al., 2018
Aulacanthidae CCE	0.07	6.01	0.4	CCE	Biard et al., 2018
Aulacanthidae CCE	0.15	12.06	0.81	CCE	Biard et al., 2018
Aulacanthidae CCE	0.14	11.19	0.75	CCE	Biard et al., 2018
Aulacanthidae CCE	0.11	7.76	0.52	CCE	Biard et al., 2018
Aulacanthidae CCE	0.11	24.76	1.66	CCE	Biard et al., 2018
Aulacanthidae CCE	0.21	22.62	1.52	CCE	Biard et al., 2018
Theoperidae	0.2	8.61	0.58	CCE	Biard et al., 2018
Theoperidae	0.14	5.47	0.37	CCE	Biard et al., 2018
Castanellidae	0.17	242.62	16.26	CCE	Biard et al., 2018
Castanellidae	0.16	225.83	15.13	CCE	Biard et al., 2018
Castanellidae	0.17	219.21	14.69	CCE	Biard et al., 2018
Castanellidae	0.16	248.29	16.64	CCE	Biard et al., 2018
Castanellidae	0.14	234.75	15.73	CCE	Biard et al., 2018
Aulosphaeridae	7.27	235.87	15.8	CCE	Biard et al., 2018
Aulosphaeridae	7.36	278.41	18.65	CCE	Biard et al., 2018
Aulosphaeridae	5.39	158.75	10.64	CCE	Biard et al., 2018
Aulosphaeridae	6.25	215.92	14.47	CCE	Biard et al., 2018
Aulosphaeridae	5.59	160.8	10.77	CCE	Biard et al., 2018
Aulosphaeridae	10.74	127.6	8.55	CCE	Biard et al., 2018
Aulosphaeridae	6.7	247.16	16.56	CCE	Biard et al., 2018
Aulosphaeridae	8.2	286.7	19.21	CCE	Biard et al., 2018
Aulosphaeridae	2.25	93.74	6.28	CCE	Biard et al., 2018
Aulosphaeridae	5.62	220.31	14.76	CCE	Biard et al., 2018
Aulosphaeridae	7.83	98.34	6.59	CCE	Biard et al., 2018
Aulosphaeridae	1.45	55.1	3.69	CCE	Biard et al., 2018
Medusettidae	26.45	648.02	43.42	CCE	Biard et al., 2018
Aulosphaeridae	5.54	107.27	7.19	CCE	Biard et al., 2018
Coelodendridae	5.6	265.72	17.8	CCE	Biard et al., 2018
Aulosphaeridae	5.7	109.09	7.31	CCE	Biard et al., 2018
Aulosphaeridae	4.86	109.09	7.31	CCE	Biard et al., 2018
Aulosphaeridae	1.53	75.69	5.07	CCE	Biard et al., 2018
Aulosphaeridae	1.56	67.61	4.53	CCE	Biard et al., 2018
Aulosphaeridae	4.02	77.85	5.22	CCE	Biard et al., 2018
Aulosphaeridae	5.4	115.49	7.74	CCE	Biard et al., 2018
Aulosphaeridae	9.67	326.86	21.9	CCE	Biard et al., 2018
Aulosphaeridae	6.72	265.72	17.8	CCE	Biard et al., 2018
Aulosphaeridae	1.41	81.18	5.44	CCE	Biard et al., 2018
Aulosphaeridae	1.61	130.5	8.74	CCE	Biard et al., 2018
Aulosphaeridae	2.42	91.59	6.14	CCE	Biard et al., 2018
Aulosphaeridae	0.94	68.57	4.59	CCE	Biard et al., 2018
Aulosphaeridae	5.45	257.99	17.29	CCE	Biard et al., 2018
Aulacanthidae CCE	0.24	39.95	2.68	CCE	Biard et al., 2018
Aulacanthidae CCE	0.3	65.52	4.39	CCE	Biard et al., 2018
Aulacanthidae CCE	0.11	52.53	3.52	CCE	Biard et al., 2018
Aulacanthidae CCE	0.13	41.05	2.75	CCE	Biard et al., 2018
Aulacanthidae CCE	0.13	41.75	2.8	CCE	Biard et al., 2018
Aulacanthidae CCE	0.14	27.73	1.86	CCE	Biard et al., 2018
Aulacanthidae CCE	0.09	52.37	3.51	CCE	Biard et al., 2018
Coelodendridae	0.21	39.95	2.68	CCE	Biard et al., 2018
Coelodendridae	0.15	39.13	2.62	CCE	Biard et al., 2018
Coelodendridae	0.15	31.6	2.12	CCE	Biard et al., 2018
Coelodendridae	0.15	31.48	2.11	CCE	Biard et al., 2018
Coelodendridae	0.18	54.64	3.66	CCE	Biard et al., 2018
Castanellidae	0.05	190.2	12.74	CCE	Biard et al., 2018
Aulosphaeridae	1.74	354.3	23.74	CCE	Biard et al., 2018
Castanellidae	0.1	243.3	16.3	CCE	Biard et al., 2018

Castanellidae	0.07	175.6	11.77	CCE	Biard et al., 2018
Aulosphaeridae	0.72	137.3	9.2	CCE	Biard et al., 2018
Castanellidae	0.05	173.6	11.63	CCE	Biard et al., 2018
Collodaria	0.0042	1.65	0.11	Med	Llopis-Monferrer et al., 2020
Collodaria	0.0023	1.04	0.07	Med	Llopis-Monferrer et al., 2020
Collodaria	0.0006	0.37	0.02	Med	Llopis-Monferrer et al., 2020
Collodaria	0.0024	0.81	0.05	Med	Llopis-Monferrer et al., 2020
Collodaria	0.0012	0.96	0.06	Med	Llopis-Monferrer et al., 2020
Collodaria	0.0013	2.63	0.18	Med	Llopis-Monferrer et al., 2020
Nassellaria	0.0003	2.15	0.14	Med	Llopis-Monferrer et al., 2020
Nassellaria	0.0003	3.23	0.22	Med	Llopis-Monferrer et al., 2020
Nassellaria	0.0003	1.08	0.07	Med	Llopis-Monferrer et al., 2020
Spumellaria	0.0031	12.64	0.85	Med	Llopis-Monferrer et al., 2020
Spumellaria	0.0037	9.27	0.62	Med	Llopis-Monferrer et al., 2020
Spumellaria	0.0006	0.81	0.05	Med	Llopis-Monferrer et al., 2020
Spumellaria	0.0004	1.62	0.11	Med	Llopis-Monferrer et al., 2020
Aulacanthidae Med.	0.2730	42.97	2.88	Med	Llopis-Monferrer et al., 2020
Aulacanthidae Med.	0.3830	23.33	1.56	Med	Llopis-Monferrer et al., 2020
Aulacanthidae Med.	0.1453	24.62	1.65	Med	Llopis-Monferrer et al., 2020
Aulacanthidae Med.	0.4943	35.51	2.38	Med	Llopis-Monferrer et al., 2020
Aulacanthidae Med.	0.3103	16.62	1.11	Med	Llopis-Monferrer et al., 2020
Aulacanthidae Med.	0.5738	29.93	2.01	Med	Llopis-Monferrer et al., 2020
Aulacanthidae Med.	0.4928	16.59	1.11	Med	Llopis-Monferrer et al., 2020
Aulacanthidae Med.	0.4604	16.83	1.13	Med	Llopis-Monferrer et al., 2020
Aulacanthidae Med.	0.1724	59.63	3.99	Med	Llopis-Monferrer et al., 2020
Aulacanthidae Med.	0.1724	16.33	1.09	Med	Llopis-Monferrer et al., 2020
Aulacanthidae Med.	0.1724	22.29	1.49	Med	Llopis-Monferrer et al., 2020
Aulacanthidae Med.	0.1724	9.39	0.63	Med	Llopis-Monferrer et al., 2020
Aulacanthidae Med.	0.4100	25.22	1.69	Med	Llopis-Monferrer et al., 2020
Aulacanthidae Med.	0.3115	24.64	1.65	Med	Llopis-Monferrer et al., 2020
Aulacanthidae Med.	0.3115	21.68	1.45	Med	Llopis-Monferrer et al., 2020
Aulacanthidae Med.	0.3115	31.58	2.12	Med	Llopis-Monferrer et al., 2020
Aulacanthidae Med.	0.3115	26.45	1.77	Med	Llopis-Monferrer et al., 2020
Protocystis Med.	0.0072	9.04	0.61	Med	Llopis-Monferrer et al., 2020
Protocystis Med.	0.0007	1.59	0.11	Med	Llopis-Monferrer et al., 2020
Protocystis Med.	0.0002	2.03	0.14	Med	Llopis-Monferrer et al., 2020
Protocystis Med.	0.0005	1.06	0.07	Med	Llopis-Monferrer et al., 2020
Protocystis Med.	0.0005	1.73	0.12	Med	Llopis-Monferrer et al., 2020

* CCE stands for California Current Ecosystem and Med for Mediterranean Sea.

4 Excess densities and sinking speeds

The excess density (μg mm^{-3}) of an organism is given by:

$$\sigma_{cell} = \rho_{cell} - \rho_{sw} \tag{2}$$

with ρ_{cell} the density of the cell and ρ_{sw} the density of seawater. For these calculations, we assumed that density of seawater was 1027.5 kg m^{-3} in the Mediterranean Sea (salinity = 37, temperature = 15°C) and 1025.2 kg m^{-3} in the California Current (salinity = 34, temperature = 15°C).

According to Baines et al. (2010) and Stukel et al. (2018), we computed the cell densities as follows:

$$\rho_{cell} = \frac{M_{cell}}{V_{cell}} \tag{3}$$

V_{cell} the cellular volume (mm^3) was expressed as:

$$V_{cell} = V_{skel} + V_{om} + V_w \tag{4}$$

V_{cell} was directly measured on photos. V_{skel} and V_{om} were deduced from the elemental mass and the assumed excess densities of 2.15 g ml^{-1} for biogenic silica and 1.05 g ml^{-1} for organic matter, i.e.:

$$V_{skel} = \frac{Q_{bSi}}{2.15 \times 10^{-3}} \tag{5}$$

$$V_{om} = \frac{Q_C + Q_N}{1.05 \times 10^{-3}} \tag{6}$$

with Q_{bSi}, Q_C and Q_N the bSi, C and N contents in μg cell^{-1}, respectively.

M_{cell} the cellular mass (μg) was expressed as:

$$M_{cell} = M_{skel} + M_{om} + M_w \tag{7}$$

with $M_{skel} = Q_{bSi}$, $M_{om} = Q_C + Q_N$ and $M_w = \rho_{sw} \times V_w$.

The theoretical sinking speeds U_{th} (in m s^{-1}) were computed from Stokes' Law (Stokes, 1851) as:

$$U_{th} = \frac{1}{18} \frac{g(\rho_{cell} - \rho_{sw}) ESD^2}{\mu_{sw}} \tag{8}$$

with $g = 9.81$ m s^2 the gravitational acceleration and $\mu_{sw} = 0.001$ Pa s the assumed dynamic viscosity of the fluid.

5 Elemental content-to-volume relationships: residual analysis

5.1 Carbon

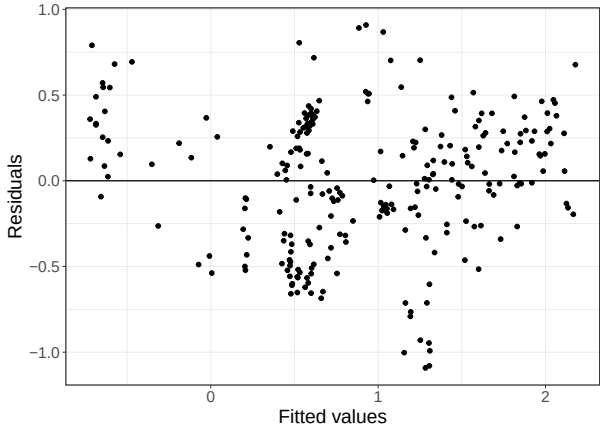

(a) Residuals as a function of fitted values

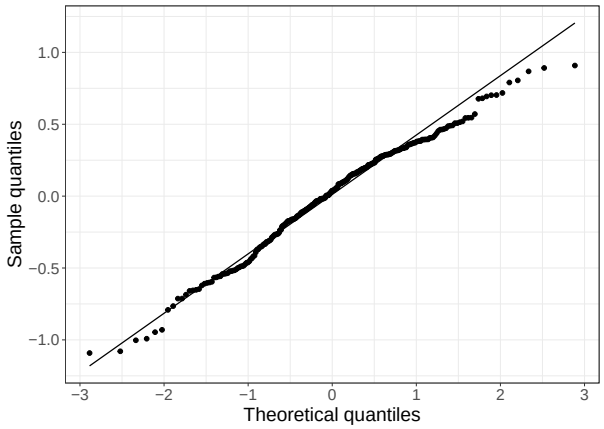

(b) Quantile-quantile plot

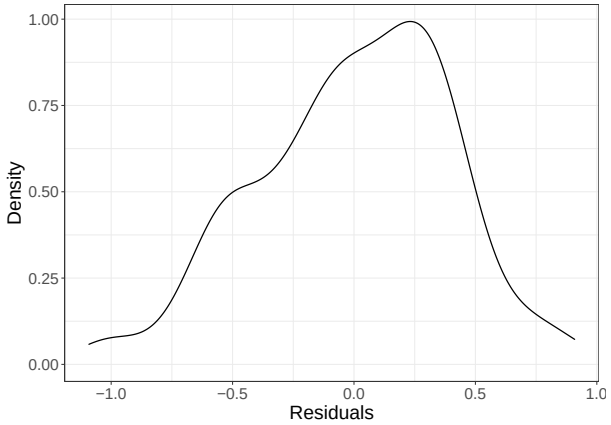

(c) Density plot of the residuals

Figure 2: Residual analysis for the model 1 least-squares regression of $\log_{10}$–transformed Q_C (μg C cell^{-1}) to V (mm^3) for Rhizaria specimens including solitary cells and colonies.

5.2 Nitrogen

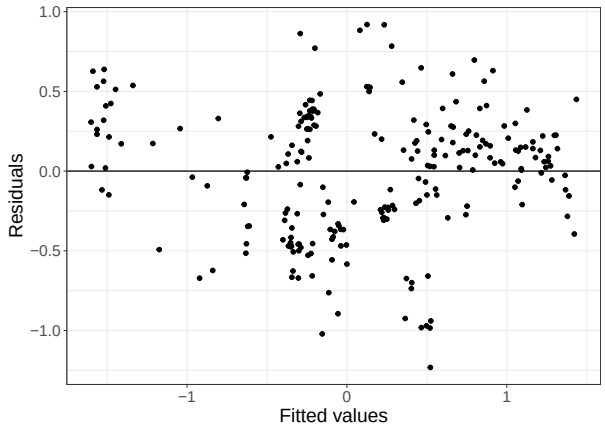

(a) Residuals as a function of fitted values

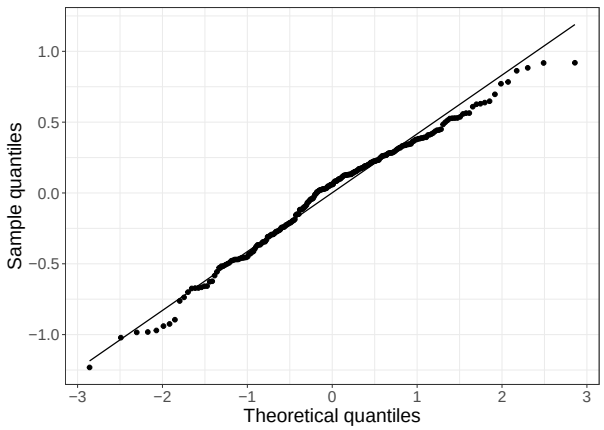

(b) Quantile-quantile plot

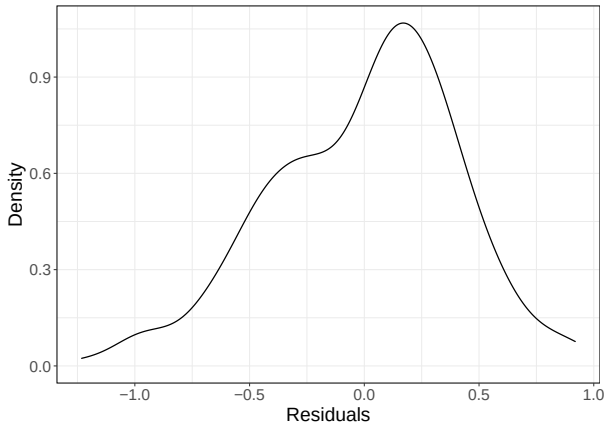

(c) Density plot of the residuals

Figure 3: Residual analysis for the model 1 least-squares regression of $\log_{10}$–transformed Q_N (μg N cell^{-1}) to V for Rhizaria specimens including solitary cells and colonies.

6 Comparison of models for Phaeodaria and Radiolaria

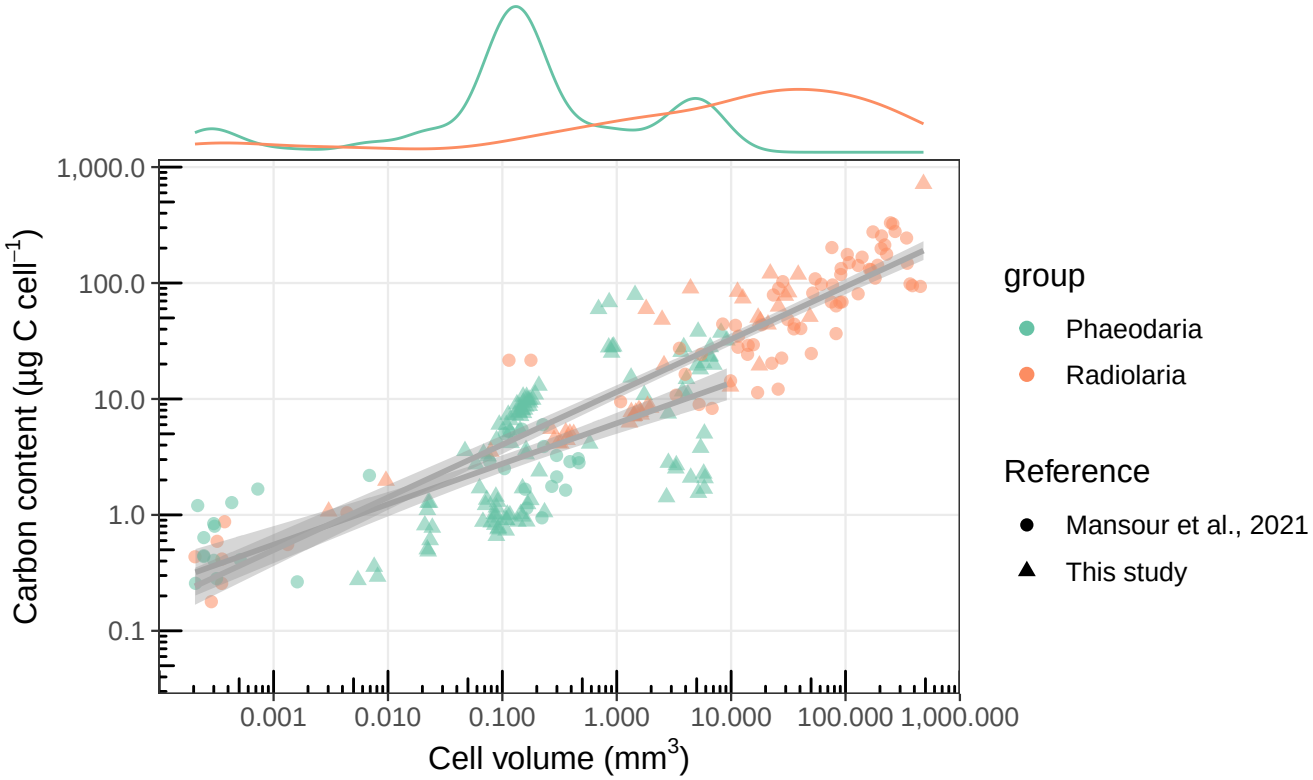

Figure 4: Model 1 least-squares regression of $\log_{10}$–transformed Q_C (μg C cell^{-1}) to V (mm^3) for Radiolaria and Phaeodaria considered separately. Grey area represents the 95% confidence level intervals for predictions. Above density plots show the repartition of data per group. Data are compiled from Mansour et al. (2021) and this study.

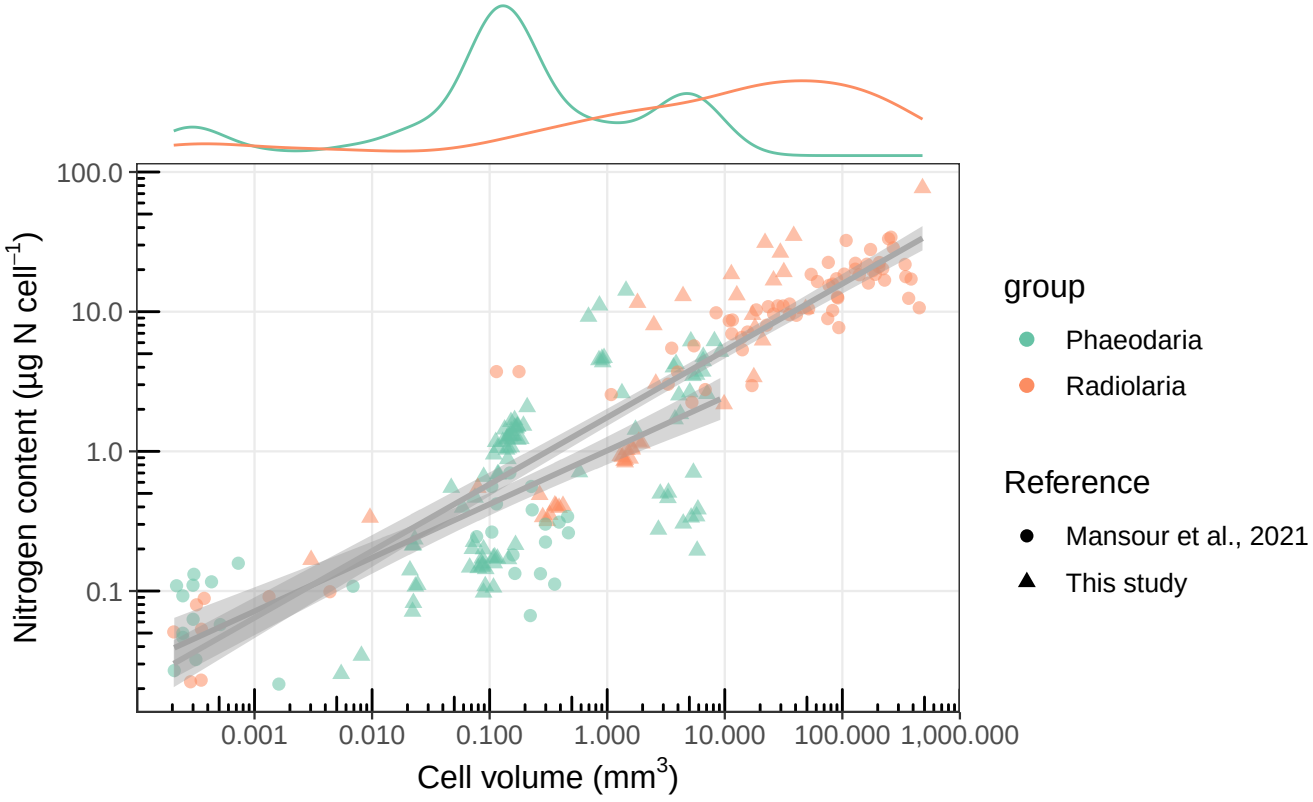

Figure 5: Model 1 least-squares regression of $\log_{10}$–transformed Q_N (μg N cell^{-1}) to V (mm^3) for Radiolaria and Phaeodaria considered separately. Grey area represents the 95% confidence level intervals for predictions. Above density plots show the repartition of data per group. Data are compiled from Mansour et al. (2021) and this study.

Table 4: Equations from models 1 ordinary least-squares regression of $\log_{10}$-transformed Q_C or Q_N (μg C cell^{-1} or μg N cell^{-1}) to V (mm^3) for Radiolaria and Phaeodaria considered separately. Data are compiled from Mansour et al. (2021) and this study.

Group	Equation	R^2
Radiolaria C	$\log_{10} Q_C = [1.06 \pm 0.03] + [0.45 \pm 0.02] \times \log_{10} V$	0.866
Phaeodaria C	$\log_{10} Q_C = [0.79 \pm 0.05] + [0.35 \pm 0.03] \times \log_{10} V$	0.435
Radiolaria N	$\log_{10} Q_N = [0.24 \pm 0.03] + [0.48 \pm 0.02] \times \log_{10} V$	0.869
Phaeodaria N	$\log_{10} Q_N = [0.01 \pm 0.05] + [0.38 \pm 0.04] \times \log_{10} V$	0.482

7 Molar C:N ratios

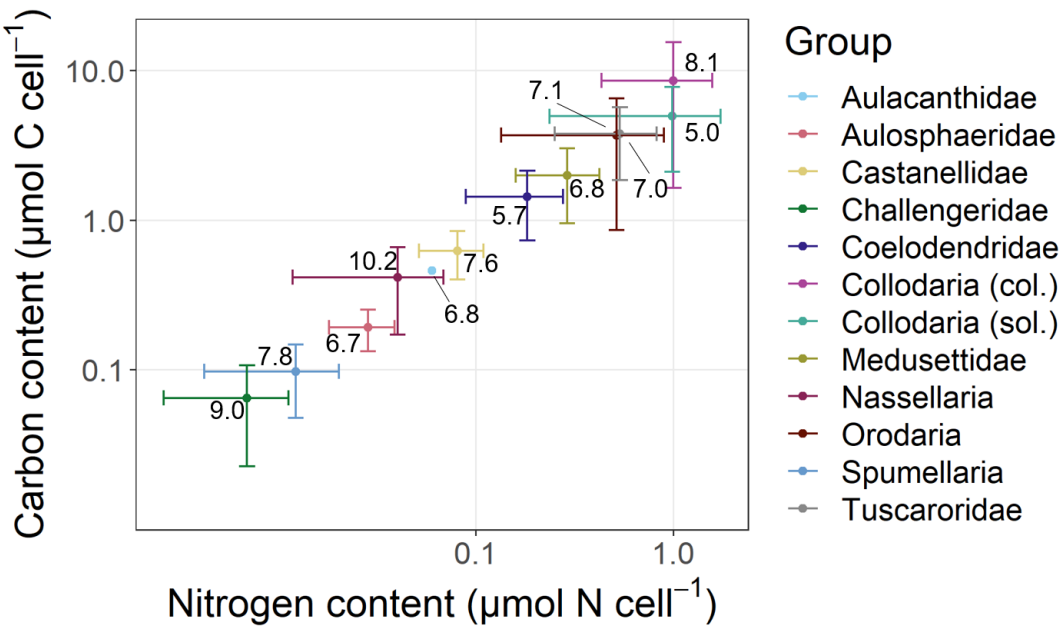

Figure 6: Mean carbon content (μmol C cell^{-1}) as a function of mean nitrogen content (μmol N cell^{-1}) for various Rhizaria taxa. Values are for each group the molar ratio of the mean carbon content to the mean nitrogen content. Error bars show mean ± standard error. Data are compiled from Mansour et al. (2021) and this study.

8 Biogenic silica content and molar Si:C ratio

8.1 Biogenic silica content to volume allometry

The previous allometry was given by (Llopis-Monferrer et al., 2020):

$$\log_{10}(Q_{bSi}) = -4.05 + 0.52 \times \log_{10}(V) \tag{9}$$

with Q_{bSi} in μg Si cell^{-1} and V in μm^3.

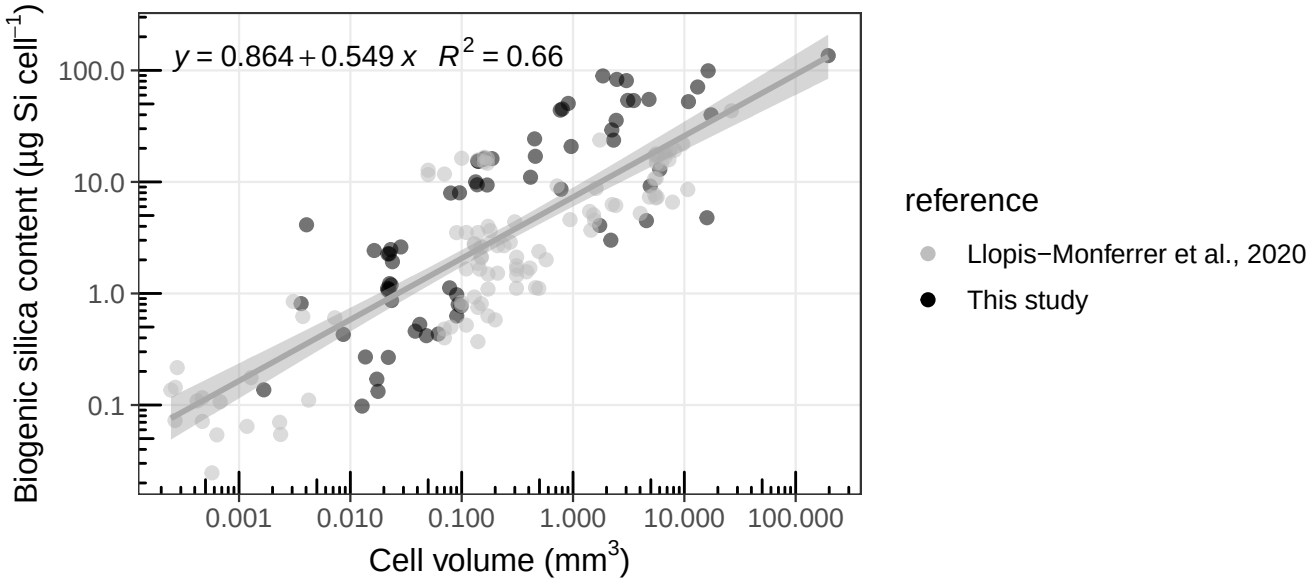

Figure 7: New model 1 least-squares regression of $\log_{10}$–transformed silica content (μg Si cell^{-1}) to cell volume (μm^3) for siliceous Rhizaria. Data are compiled from Llopis-Monferrer et al. (2020) and this study.

8.2 Molar Si:C ratio

Table 5: Summary of carbon and biogenic silica contents. Si:C ratio are calculated as the ratio of the median silica content to the median carbon content. Data are compiled from Biard et al. (2018), Llopis-Monferrer et al. (2020), Mansour et al. (2021) and this study.

Group	Taxon	Area*	n_C	Median nmol C cell^{-1}	Range nmol C cell^{-1}	n_{bSi}	Median nmol Si cell^{-1}	Range nmol Si cell^{-1}	Si:C
Phaeodaria	Aulacanthidae	CCE	24	84	54–3114	32	26	6–1479	0.31
	Aulacanthidae	Med	27	208	78–500	17	24	9–59	0.12
	Aulosphaeridae	CCE	10	182	118–316	34	129	44–595	0.71
	Castanellidae	CCE	35	640	112–1086	19	225	118–248	0.35
	Coelodendridae	CCE	13	970	73–2337	10	60	31–819	0.06
	Medusettidae	CCE	3	1504	1277–3179	1	648	648–648	0.43
	Challegenridae (*Protocystis* sp.)	CCE	11	50	22–106	13	17	6–39	0.34
	Tuscaroridae	CCE	7	2367	2093–6596	7	656	164–1331	0.28
Radiolaria	Nassellaria (*Phlebarachnium* sp.)	CCE	19	589	343–730	10	4	1–7	0.01
	Orodaria (*Oroscena* sp.)	CCE	5	4029	292–7507	2	654	71–1238	0.16
	Spumellaria	CCE	2	126	89–164	1	61	61–61	0.48

* CCE stands for California Current Ecosystem and Med for Mediterranean Sea.

9 Silicon uptake rates ρ_{Si}

Table 6: Summary data of biogenic Si contents (Q_{bSi}), Si uptake rates (ρ_{Si}) and Si specific uptake rates (V_{Si}) from this study.

Group	Taxon	n	ESD[1,2] (μm)	Q_{bSi} [1] (nmol Si cell^{-1})	ρ_{Si} [1] (nmol Si cell^{-1} d^{-1})	V_{Si} [1] (d^{-1})
Phaeodaria	Aulacanthidae	4	832 ± 558	142.52 ± 259.73	0.46 ± 0.70	0.0077 ± 0.0079
	Aulosphaeridae	6	1948 ± 736	193.37 ± 204.47	0.62 ± 0.54	0.0056 ± 0.0074
	Castanellidae	3	655 ± 43	232.95 ± 7.33	0.17 ± 0.11	0.0007 ± 0.0005
	Challegenridae (*Protocystis* sp.)	1	353	36.95	0.07	0.0020
Radiolaria	Collodaria	1	7209	2024.30	4.31	0.0021
	Nassellaria (*Phlebarachnium* sp.)	10	346 ± 99	4.35 ± 2.35	0.31 ± 0.25	0.0647 ± 0.0350
	Orodaria (*Oroscena* sp.)	1	1678	1238.69	0.81	0.0007

[1] Values are expressed as mean ± standard error. [2] Equivalent Spherical Diameter.

Table 7: Daily averaged silicic acid concentration measured from sample collected with Niskin bottles.

Date (GMT)	Silicic acid conc. (μmol L^{-1})	Minimum depth (m)	Maximum depth (m)
18/07/2021	14.96400	5.495	80.958
24/07/2021	20.88050	3.738	522.860
25/07/2021	20.13625	4.832	519.776
29/07/2021	21.78250	5.015	518.891
30/07/2021	17.63312	4.737	519.135
03/08/2021	12.05937	4.721	522.432
04/08/2021	11.84625	5.311	519.642
06/08/2021	12.29625	5.488	520.188
10/08/2021	17.55813	5.392	204.520

Table 8: Detailed data and metadata of biogenic Si contents (Q_{bSi}), Si uptake rates (ρ_{Si}) and Si specific uptake rates (V_{Si}) from this study.

Latitude	Longitude	Gear	Date	Depth range (m)	Taxon	n^1	ESD^2 (μm)	Volume (μm^3)	ρ_{Si} (nmol Si cell^{-1} d^{-1})	Q_{bSi} (nmol Si cell^{-1})	V_{Si} (d^{-1})
		DeepNet	18/07/2021	1000 - 50	Aulosphaeridae	2	1606	2187105107	0.92	0.045	0.0205
36.3241	-122.7686	RingNet	24/07/2021	500 - 0	Aulacanthidae	14	561	98737338	0.22	0.012	0.0192
36.3241	-122.7686	RingNet	24/07/2021	500 - 0	Aulacanthidae	1	1671	2443025342	1.50	0.532	0.0028
36.3241	-122.7686	RingNet	24/07/2021	500 - 0	Castanellidae	4	643	141379762	0.30	0.228	0.0013
36.3241	-122.7686	RingNet	24/07/2021	500 - 0	Aulosphaeridae	4	1121	780518746	0.58	0.128	0.0045
36.3241	-122.7686	RingNet	24/07/2021	500 - 0	Aulosphaeridae	1	3215	17399004222	1.54	0.596	0.0026
36.1676	-122.4665	Mocness	25/07/2021	600 - 400	*Protocystis* sp.	5	353	23088581	0.07	0.037	0.0020
36.6044	-123.4352	Bongo	29/07/2021	300 - 0	Aulacanthidae	15	554	93152137	0.07	0.012	0.0063
36.6044	-123.4352	Bongo	29/07/2021	300 - 0	Aulacanthidae	18	546	90229089	0.04	0.015	0.0025
36.6044	-123.4352	Bongo	29/07/2021	300 - 0	Aulosphaeridae	3	1490	1737189540	0.23	0.061	0.0038
36.6044	-123.4352	Bongo	29/07/2021	300 - 0	Castanellidae	5	620	139534319	0.12	0.230	0.0005
36.6044	-123.4352	Bongo	29/07/2021	300 - 0	Orodaria	1	1678	2474195264	0.81	1.239	0.0007
36.705	-123.0394	RingNet	30/07/2021	300 - 0	Aulosphaeridae	13	2014	4939335975	0.10	0.137	0.0007
36.705	-123.0394	RingNet	30/07/2021	300 - 0	Castanellidae	9	704	187127543	0.10	0.241	0.0004
34.7136	-130.5414	RingNet	03/08/2021	50 - 0	Nassellaria	25	144	1669750	0.24	0.002	0.1185
34.7136	-130.5414	RingNet	03/08/2021	50 - 0	Nassellaria	25	293	13655738	0.25	0.004	0.0613
34.7136	-130.5414	RingNet	03/08/2021	300 - 0	Nassellaria	25	428	42002596	0.46	0.008	0.0580
34.7136	-130.5414	RingNet	03/08/2021	300 - 0	Nassellaria	25	412	38251196	0.51	0.007	0.0744
34.6385	-130.5178	RingNet	04/08/2021	50 - 0	Nassellaria	25	282	12748444	0.07	0.001	0.0505
34.6385	-130.5178	RingNet	04/08/2021	50 - 0	Nassellaria	30	316	17736047	0.06	0.002	0.0297
34.6385	-130.5178	RingNet	04/08/2021	300 - 0	Nassellaria	25	446	48186747	0.63	0.006	0.1004
34.6385	-130.5178	RingNet	04/08/2021	300 - 0	Nassellaria	25	484	61693415	0.70	0.006	0.1075
34.5029	-130.4235	RingNet	06/08/2021	300 - 0	Nassellaria	20	344	21931830	0.10	0.004	0.0256
34.5029	-130.4235	RingNet	06/08/2021	300 - 0	Nassellaria	20	317	17296937	0.05	0.003	0.0212
35.2885	-121.3928	SalpNet	10/08/2021	350 - 0	Collodaria	1	7209	1.96166E+11	4.31	2.024	0.0021
35.2885	-121.3928	SalpNet	10/08/2021	350 - 0	Aulosphaeridae	6	2248	6015315528	0.32	0.193	0.0017

[1] Number of specimens per sample. [2] Equivalent Spherical Diameter.

References

Baines, S. B., B. S. Twining, M. A. Brzezinski, D. M. Nelson, and N. S. Fisher (2010). Causes and biogeochemical implications of regional differences in silicification of marine diatoms. In: *Global Biogeochemical Cycles* 24.4 (cit. on p. 4).

Biard, T., J. W. Krause, M. R. Stukel, and M. D. Ohman (2018). The Significance of Giant Phaeodarians (Rhizaria) to Biogenic Silica Export in the California Current Ecosystem. In: *Global Biogeochemical Cycles* 32.6, pp. 987–1004. DOI: 10.1029/2018gb005877 (cit. on pp. 2–4, 12).

Llopis-Monferrer, N., D. Boltovskoy, P. Tréguer, M. M. Sandin, F. Not, and A. Leynaert (2020). Estimating Biogenic Silica Production of Rhizaria in the Global Ocean. In: *Global Biogeochemical Cycles* 34.3. DOI: 10.1029/2019gb006286 (cit. on pp. 4, 10–12).

Mansour, J. S., A. Norlin, N. Llopis Monferrer, S. l'Helguen, and F. Not (2021). Carbon and nitrogen content to biovolume relationships for marine protist of the Rhizaria lineage (Radiolaria and Phaeodaria). In: *Limnology and Oceanography* 66.5, pp. 1703–1717 (cit. on pp. 8–10, 12).

Stokes, G. G. (1851). On the effect of the internal friction of fluids on the motion of pendulums. Vol. 9. Trans. Cambridge Philos. Soc. (cit. on p. 5).

Stukel, M. R., T. Biard, J. Krause, and M. D. Ohman (2018). Large Phaeodaria in the twilight zone: Their role in the carbon cycle. In: *Limnology and Oceanography* 63.6, pp. 2579–2594 (cit. on p. 4).